Integrated Sensing and Communication Empowered Secure Computation Offloading in Integrated Satellite-Terrestrial Networks

Chenglong Dou[1], Xumin Huang[1], Jiawen Kang[2], Yuan Wu[1,3(✉)], and Liping Qian[4]

[1] State Key Laboratory of Internet of Things for Smart City, University of Macau, Macau, China

[2] School of Automation, Guangdong University of Technology, Guangzhou 510006, China
kavinkang@gdut.edu.cn

[3] Zhuhai UM Science and Technology Research Institute, Zhuhai 519301, China
yuanwu@um.edu.mo

[4] College of Information Engineering, Zhejiang University of Technology, Hangzhou 310023, China
lpqian@zjut.edu.cn

Abstract. Integrated satellite-terrestrial edge computing networks have emerged as a promising solution to enhance data processing capabilities and connectivity in remote and underserved areas. However, the physical layer security of computation offloading in such networks is increasingly challenged by potential eavesdroppers. In this paper, we propose an integrated sensing and communication (ISAC) empowered secure computation offloading in integrated satellite-terrestrial networks, in which the satellite can utilize the ISAC signal to sense the malicious eavesdropper with an uncertain location while offloading data with improved secrecy rates. To investigate this problem, we formulate a joint optimization of the transmit beamforming, the receive beamforming, the computation offloading strategies and the associated allocations of the communication and computing resources, with the objective of maximizing the minimum sensing performance for all possible eavesdropper locations, while guaranteeing the secrecy offloading transmission rate. Despite the nonconvexity of the formulated problem, we propose an efficient algorithm to obtain its solutions. Numerical results validate the performance advantages of our ISAC empowered secure computation offloading in secrecy and robustness.

Keywords: Integrate satellite-terrestrial networks · Edge computing · Integrated sensing and communication · Physical layer security

H.-H. Chen and W. Meng (Eds.): WiSATS 2024, LNICST 605, pp. 255–268, 2025.
https://doi.org/10.1007/978-3-031-86196-3_22

1 Introduction

With the rapid development of satellite communication and edge computing technologies, integrated satellite-terrestrial networks have emerged as a promising solution to enhance data processing capabilities and provide seamless connectivity, especially in remote and underserved areas [1]. These networks leverage the unique advantages of low Earth orbit (LEO) satellites and terrestrial infrastructures to support a wide range of applications such as real time data analytics. However, the proliferation of such networks also poses significant security challenges, especially in the case of computation offloading of privacy sensitive data [2].

With the increased computation capacity of eavesdroppers, traditional secure communications based on cryptographic techniques in the upper layers of the protocol stack become increasingly unreliable. To this end, physical layer security approaches have been proposed as the promising solution, particularly in integrated satellite-terrestrial networks [3]. Numerous studies have demonstrated the effectiveness of physical layer security in improving communication confidentiality and eavesdropping resistance. In [4], Liu *et al.* proposed an access authentication protocol in integrated satellite-terrestrial networks with user anonymity and traceability. In [5], An *et al.* proposed to employ the source of green interference to enhance secure transmission in integrated satellite-terrestrial networks. In [6], Lin *et al.* investigated secrecy energy efficient hybrid beamforming schemes for integrated satellite-terrestrial networks. Nevertheless, due to the unpredictable locations of eavesdroppers, the above approaches are insufficient to address the security challenges comprehensively. Thus, a more adaptable security solution is necessitated.

Integrated sensing and communication (ISAC), which allows simultaneous transmission and sensing on the same resource block, provides a promising avenue for dynamically adapting to the presence of eavesdroppers and obtaining their accurate information [7]. Due to its great potential, ISAC attracts wide research interests for various wireless services [8–10]. In this paper, we propose an ISAC empowered secure computation offloading in integrated satellite-terrestrial networks. By deploying ISAC on the LEO satellite, it can simultaneously perform data offloading and eavesdropper detection. The integration of sensing capabilities allows the satellite to accurately locate potential eavesdroppers and adapt its computation offloading strategies accordingly. Moreover, the use of dedicated sensing signal not only aids in eavesdropper detection but also generates intentional interference, which further protects the offloaded data from interception. Our contributions can be summarized as follows.

- We propose an ISAC empowered secure computation offloading in the integrated satellite-terrestrial network, in which the satellite can utilize the ISAC signal to sense the malicious eavesdropper with an uncertain location while offloading data with improved secrecy rates.
- We formulate a joint optimization problem with the objective of maximizing the minimum sensing performance for all possible eavesdropper locations,

while guaranteeing the secrecy offloading transmission rate. We design the surrogate functions and present a convex surrogate problem for this nonconvex problem, based on which we propose an efficient algorithm for solving it.

– We present the numerical results to verify the performance superiority of leveraging ISAC for secure computation offloading in integrated satellite-terrestrial networks. The results demonstrate that our scheme outperforms the benchmark schemes in both secrecy and robustness.

The remainder of this paper is organized as follows. Section 2 depicts the system model and problem formulation. Section 3 proposes an efficient algorithm for solving the formulated problem. Section 4 presents the numerical results. Section 5 concludes this work and discusses the future directions.

2 System Model and Problem Formulation

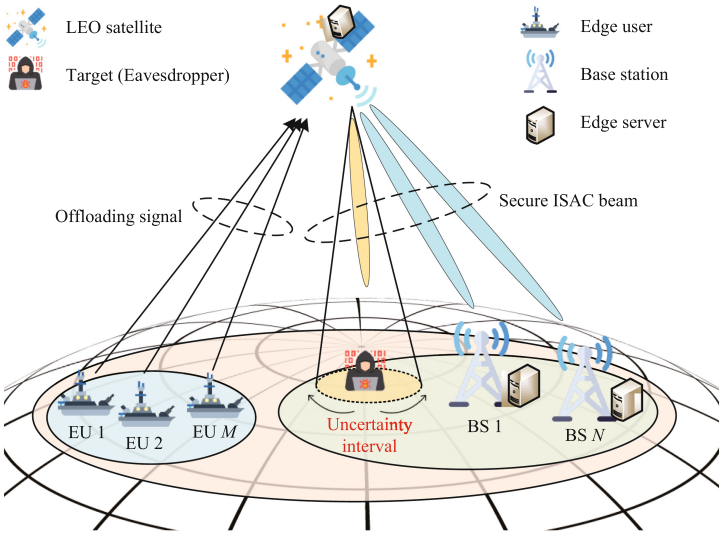

Fig. 1. Illustrative system model

As shown in Fig. 1, we consider an ISAC empowered integrated satellite-terrestrial edge computing network, which includes an LEO satellite with N_t transmit antennas and N_r receive antennas, a group of edge users (EUs) represented by $\mathcal{M} = \{1, 2, ..., M\}$, and a group of base stations (BSs) with N_r receive antennas represented by $\mathcal{N} = \{1, 2, ..., N\}$. In this network, the LEO satellite provides the computational task offloading services for the EUs (e.g., the unmanned surface vehicles), and it can further offload the workloads to the

BSs for efficient processing. Furthermore, we consider the presence of a potential malicious eavesdropper with an uncertain location that may intercept the data offloaded by the LEO satellite. To achieve secure computation offloading, ISAC is deployed on the LEO satellite to sense the location of the eavesdropper and prevent information leakage while offloading to the BSs.

2.1 Signal Model

In this work, we consider that the EUs offload their entire task workloads $\{D_m^{\text{tot}}\}_{m\in\mathcal{M}}$ to the LEO satellite due to their limited computation capacities. The transmitted signal of EU m is given by

$$x_m = \sqrt{p_m} s_m, \tag{1}$$

where p_m denotes the transmit power for delivering the information symbol s_m with $\mathbb{E}\{|s_m|^2\} = 1$. The task workloads at the LEO satellite can be further offloaded to a group of BSs via the ISAC signal. The transmitted ISAC signal of the LEO satellite is given by

$$\mathbf{x} = \sum_{n\in\mathcal{N}} \mathbf{u}_n z_n + \mathbf{v}_0, \tag{2}$$

where $\mathbf{u}_n \in \mathbb{C}^{N_t\times 1}$ denotes the transmit beamforming for BS n, and z_n with $\mathbb{E}\{|z_n|^2\} = 1$ denotes the symbol for BS n. In Eq. (2), $\mathbf{v}_0$ denotes the dedicated sensing signal, which is exploited to enhance the sensing performance towards the eavesdropper and serve as a jamming to the eavesdropper.

We consider that the uncertainty interval of the eavesdropper is $\theta_0 \in \Phi = [\theta_e - \Delta\theta, \theta_e + \Delta\theta]$, and there exists I clutters under the angles of $\{\theta_i\}_{i=1}^I$. The received signal at the LEO satellite consists of three parts, including the offloading signal from M EUs, the sensing echo from the eavesdropper, and the clutter interference from I clutters and noise. It can be expressed as

$$\begin{aligned}\mathbf{y}_0 = &\underbrace{\sum_{m\in\mathcal{M}} \mathbf{h}_m \sqrt{p_m} s_m}_{\text{signal from all EUs}} + \underbrace{\kappa_0 \mathbf{a}_r(\theta_0)\mathbf{a}_t^H(\theta_0)\mathbf{x}}_{\text{sensing echo from the eavesdropper}} \\ &+ \underbrace{\sum_{i=1}^{I} \kappa_i \mathbf{a}_r(\theta_i)\mathbf{a}_t^H(\theta_i)\mathbf{x} + \mathbf{n}_0}_{\text{clutter interference and noise}},\end{aligned} \tag{3}$$

where $\mathbf{h}_m \in \mathbb{C}^{N_r\times 1}$ denotes the channel from EU m to the LEO satellite. The complex amplitudes $\{\kappa_i\}_{i=0,1,\ldots,I}$ are primarily determined by the factors such as the path loss and radar cross section. $\mathbf{n}_0$ denotes the noise with variance σ_0^2. In Eq. (3), $\mathbf{a}_t(\theta)$ and $\mathbf{a}_r(\theta)$ are the steering vectors of uniform linear array antenna with half wavelength antenna spacing, and can be respectively defined as

$$\mathbf{a}_t(\theta) = \frac{1}{\sqrt{N_t}} \left[1, e^{j\pi\sin\theta}, \ldots, e^{j\pi(N_t-1)\sin\theta}\right]^T, \tag{4}$$

$$\mathbf{a}_r(\theta) = \frac{1}{\sqrt{N_r}} \left[1, e^{j\pi \sin\theta}, ..., e^{j\pi(N_r-1)\sin\theta}\right]^T. \tag{5}$$

For the sake of clear notations, we further define $\mathbf{A}_s = \kappa_0 \mathbf{a}_r(\theta_0)\mathbf{a}_t^H(\theta_0)$ and $\mathbf{A}_c = \sum_{i=1}^{I} \kappa_i \mathbf{a}_r(\theta_i)\mathbf{a}_t^H(\theta_i)$.

We use $\mathbf{G}_n \in \mathbb{C}^{N_r \times N_t}$ to denote the channel from the LEO satellite to BS n. Then, the received signal at BS n can be expressed as

$$\mathbf{y}_n = \mathbf{G}_n \mathbf{u}_n z_n + \sum_{j \in \mathcal{N}, j \neq n} \mathbf{G}_n \mathbf{u}_j z_j + \mathbf{n}_n, \tag{6}$$

where n_n denotes the noise with variance σ_n^2.

2.2 Computation Offloading Model

Based on Eq. (3), the offloading transmission rate from EU m to the LEO satellite is given by

$$R_m^u = B^u \log_2 \left(1 + \frac{p_m \mathbf{c}_m^H \mathbf{h}_m \mathbf{h}_m^H \mathbf{c}_m}{\mathbf{c}_m^H \mathbf{\Gamma}_m \mathbf{c}_m}\right), \tag{7}$$

where B^u denotes the channel bandwidth between the EUs and LEO satellite, and $\mathbf{c}_m \in \mathbb{C}^{N_r \times 1}$ denotes the LEO satellite's receive beamforming for EU m's data. In Eq. (7), $\mathbf{\Gamma}_m$ denotes the total interference for receiving EU m's data, and it can be expressed as

$$\mathbf{\Gamma}_m = \sum_{j \in \mathcal{M}, j \neq m} p_j \mathbf{h}_j \mathbf{h}_j^H + (\mathbf{A}_s + \mathbf{A}_c)\, \mathbf{x}\mathbf{x}^H \left(\mathbf{A}_s^H + \mathbf{A}_c^H\right) + \sigma_0^2 \mathbf{I}_N. \tag{8}$$

According to the minimum variance distortionless response (MVDR) beamforming problem, the optimal receiver $\mathbf{c}_m^*$ is given by

$$\mathbf{c}_m^* = \arg\max \frac{p_m \mathbf{c}_m^H \mathbf{h}_m \mathbf{h}_m^H \mathbf{c}_m}{\mathbf{c}_m^H \mathbf{\Gamma}_m \mathbf{c}_m} = \mathbf{\Gamma}_m^{-1} \mathbf{h}_m, \forall m \in \mathcal{M}. \tag{9}$$

By substituting $\mathbf{c}_m^*$ into Eq. (7), the offloading transmission rate R_m^u can be rewritten as

$$R_m^u = B^u \log_2 \left(1 + p_m \mathbf{h}_m^H \mathbf{\Gamma}_m^{-1} \mathbf{h}_m\right), \forall m \in \mathcal{M}. \tag{10}$$

We use B^d to denote the channel bandwidth between the LEO satellite and the BSs. Based on Eq. (6), the offloading transmission rate from the LEO satellite to BS n is given by

$$R_n^d = B^d \log_2 \left(1 + \frac{\mathbf{q}_n^H \mathbf{G}_n \mathbf{u}_n \mathbf{u}_n^H \mathbf{G}_n^H \mathbf{q}_n}{\mathbf{q}_n^H \mathbf{\Lambda}_n \mathbf{q}_n}\right), \tag{11}$$

where $\mathbf{q}_n \in \mathbb{C}^{N_r \times 1}$ denotes the receive beamforming of BS n. $\mathbf{\Lambda}_n$ is the inference of BS n for receiving the offloaded workloads from the LEO satellite, and it can be expressed as

$$\mathbf{\Lambda}_n = \mathbf{G}_n \left(\sum_{j \in \mathcal{N}, j \neq n} \mathbf{u}_j \mathbf{u}_j^H\right) \mathbf{G}_n^H + \mathbf{G}_n \mathbf{v}_0 \mathbf{v}_0^H \mathbf{G}_n^H + \sigma_n^2. \tag{12}$$

The optimal receiver $\mathbf{q}_n^*$ is given by

$$\mathbf{q}_n^* = \arg\max \frac{\mathbf{q}_n^H \mathbf{G}_n \mathbf{u}_n \mathbf{u}_n^H \mathbf{G}_n^H \mathbf{q}_n}{\mathbf{q}_n^H \mathbf{\Lambda}_n \mathbf{q}_n} = \frac{\mathbf{\Lambda}_n^{-1} \mathbf{G}_n \mathbf{u}_n}{\mathbf{u}_n^H \mathbf{G}_n^H \mathbf{\Lambda}_n^{-1} \mathbf{G}_n \mathbf{u}_n}. \tag{13}$$

By substituting $\mathbf{q}_n^*$ into Eq. (11), the offloading transmission rate R_n^d can be rewritten as

$$R_n^d = B^d \log_2 \left(1 + \mathbf{u}_n^H \mathbf{G}_n^H \mathbf{\Lambda}_n^{-1} \mathbf{G}_n \mathbf{u}_n\right), \forall n \in \mathcal{N}. \tag{14}$$

The latency for completing EU m's workloads is determined by two parts, including the latency l_m^{LS} for processing at the LEO satellite, and the latency l_m^{BS} for processing at the BSs. We use d_{mn} to denote the EU m's workloads offloaded from the LEO satellite to BS n. The latency for processing EU m's workloads at the LEO satellite is given by

$$l_m^{\mathrm{LS}} = \frac{D_m^{\mathrm{tot}}}{R_m^u} + \frac{\nu_m (D_m^{\mathrm{tot}} - \sum_{n \in \mathcal{N}} d_{mn})}{\varrho_m}, \tag{15}$$

where ν_m denotes the number of CPU cycles for processing one bit of D_m^{tot}, and ϱ_m denotes the processing rate of the LEO satellite for processing EU m's offloaded workloads. We use t_n to denote the transmission duration from the LEO satellite to BS n. The latency for processing EU m's workloads at the BSs is given by

$$l_m^{\mathrm{BS}} = \frac{D_m^{\mathrm{tot}}}{R_m^u} + \max_{n \in \mathcal{N}} \{t_n + \frac{\nu_m d_{mn}}{\zeta_{mn}}\}, \tag{16}$$

where ζ_{mn} denotes the processing rate of BS n allocated for processing the offloaded workloads from EU m.

The power consumption of the LEO satellite can be expressed as

$$P_0 = \sum_{n \in \mathcal{N}} \mathbf{u}_n^H \mathbf{u}_n + \mathbf{v}_0^H \mathbf{v}_0 + \sum_{m \in \mathcal{M}} \epsilon_0 \varrho_m^3, \tag{17}$$

where ϵ_0 denotes the power consumption coefficient of the LEO satellite.

2.3 Sensing and Interception Model

With the sensing receive beamforming $\mathbf{w}$, the output sensing SINR is given by

$$\mathrm{SINR}(\theta_0) = \frac{\mathbf{w}^H \mathbf{A}_s \mathbf{x}\mathbf{x}^H \mathbf{A}_s^H \mathbf{w}}{\mathbf{w}^H (\mathbf{A}_c \mathbf{x}\mathbf{x}^H \mathbf{A}_c^H + \sigma_0^2 \mathbf{I}_N) \mathbf{w}}. \tag{18}$$

Due to the presence of the potential malicious eavesdropper, the data offloaded by the LEO satellite is at risk of leakage. We use $\mathbf{\Theta}$ to denote the estimated channel from the LEO satellite to the eavesdropper. Considering the uncertainty of target location, the bounded channel state information (CSI) error for $\mathbf{\Theta}$ is given by

$$\mathbf{\Theta} = \overline{\mathbf{\Theta}} + \Delta\mathbf{\Theta}, \Delta\mathbf{\Theta} \in \mathcal{J}_{\mathbf{\Theta}} = \{||\Delta\mathbf{\Theta}||_F \leq \varepsilon\}. \tag{19}$$

The received SINR at the eavesdropper for intercepting the data offloaded from the LEO satellite to BS n is expressed as

$$\gamma_n^e = \frac{|\mathbf{\Theta}^H \mathbf{u}_n|^2}{\sum_{j\in\mathcal{N}, j\neq n} |\mathbf{\Theta}^H \mathbf{u}_j|^2 + |\mathbf{\Theta}^H \mathbf{v}_0|^2 + \sigma_e^2}. \tag{20}$$

2.4 Coverage Model

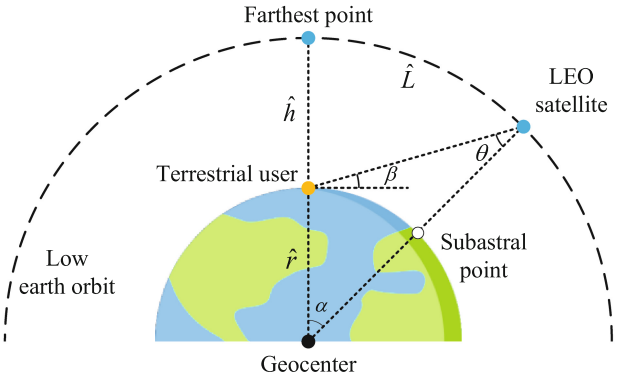

Fig. 2. Space geometric relationship

Different from the terrestrial edge computing networks, the communication link between the EUs and the LEO satellite is available only if the EUs are within the coverage area of the LEO satellite. Figure 2 shows the space geometric relationship between the EUs and the LEO satellite. In Fig. 2, $\hat{h}$ denotes the distance between the terrestrial user and the LEO, $\hat{r}$ denotes the radius of the earth, β denotes the elevation angle between the terrestrial user and the LEO satellite, α denotes the geocentric angle of the LEO satellite coverage area. After some math manipulations, α can be given by

$$\alpha = \arccos\left(\frac{\hat{r}}{\hat{r}+\hat{h}}\cos\beta\right) - \beta. \tag{21}$$

Then, the distance $\hat{L}$ from the LEO satellite to the farthest orbital point where it can maintain the available communication link with terrestrial users can be expressed as

$$\hat{L} = 2 \cdot (\hat{r} + \hat{h}) \cdot \alpha. \tag{22}$$

Based on the above model, the available communication duration for computation offloading of EU m is given by

$$T_m = \frac{\hat{L}_m}{v_s}, \tag{23}$$

where v_s denotes the speed of the LEO satellite.

2.5 Problem Formulation

To guarantee the secure computation offloading (SCO) in integrated satellite-terrestrial networks with the location uncertain malicious eavesdropper, the objective of this paper is to maximize the minimum sensing SINR for all possible eavesdropper locations within Φ, while maintaining the secrecy offloading transmission rate of the LEO satellite. To accomplish this objective, we jointly optimize the transmit beamforming $\{\mathbf{u}_n\}_{\forall n}$ and $\mathbf{v}_0$, the sensing receive beamforming $\mathbf{w}$, the offloading strategies $\{d_{mn}\}_{\forall m,n}$ of the LEO satellite for EUs' workloads, the offloading durations $\{t_n\}_{\forall n}$ from the LEO satellite to the BSs, and the computation rate $\{\varrho_m\}_{\forall m}$ allocated by the LEO satellite as follows.

$$
\begin{aligned}
\text{(SCO):}\ \max\ & \min_{\theta_0 \in \Phi}\ \mathrm{SINR}(\theta_0) \\
\text{subject to:}\ & \max\{l_m^{\mathrm{LS}}, l_m^{\mathrm{BS}}\} \le T_m, \forall m \in \mathcal{M}, && (24)\\
& \gamma_n^e \le \gamma_n^{e,\max}, \forall n \in \mathcal{N}, \Delta\boldsymbol{\Theta} \in \mathcal{J}_{\boldsymbol{\Theta}}, && (25)\\
& R_n^d \ge R_n^{d,\min}, \forall n \in \mathcal{N}, && (26)\\
& R_n^d t_n \ge \sum_{m \in \mathcal{M}} d_{mn}, \forall n \in \mathcal{N}, && (27)\\
& 0 \le \sum_{n \in \mathcal{N}} d_{mn} \le D_m^{\mathrm{tot}}, \forall m \in \mathcal{M}, && (28)\\
& P_0 \le P_0^{\max}, && (29)\\
\text{variables:}\ & \{\mathbf{u}_n\}_{\forall n}, \mathbf{v}_0, \mathbf{w}, \{d_{mn}\}_{\forall m,n}, \{t_n\}_{\forall n}, \text{ and } \{\varrho_m\}_{\forall m}.
\end{aligned}
$$

Constraint (24) guarantees that the overall latency in completing EU m's workloads cannot exceed the maximum available communication duration T_m. Constraint (25) represents the maximum tolerable leakage for the computation offloading. Constraint (26) represents the minimum offloading transmission rate required by the BSs. Constraint (29) provides an upper bound for the LEO satellite's power consumption. Notice that the secrecy offloading transmission rate for BS n can be guaranteed by constraints (25) and (26), and it is bounded by $R_n^{d,\min} - \log_2(1 + \gamma_n^{e,\max})$.

3 Proposed Algorithms

It can be identified that Problem (SCO) is a strictly nonconvex optimization problem due to the fractional objective function and the strong coupling of the variables. Thus, it is very difficult to be solved directly. We next transform Problem (SCO) into a tractable form.

After some math manipulations, constraint (24) can be transformed into the following two inequalities.

$$
\frac{D_m^{\mathrm{tot}}}{T_m - \frac{\nu_m (D_m^{\mathrm{tot}} - \sum_{n \in \mathcal{N}} d_{mn})}{\varrho_m}} - R_m^u \le 0, \forall m \in \mathcal{M}, \tag{30}
$$

$$\frac{D_m^{\text{tot}}}{T_m - t_n - \frac{\nu_m d_{mn}}{\zeta_{mn}}} - R_m^u \leq 0, \forall m \in \mathcal{M}, \forall n \in \mathcal{N}. \tag{31}$$

By observing Problem (SCO) with constraints (30) and (31), we conclude that given the other variables, the optimal solutions of the sensing receive beamforming $\mathbf{w}^*$ and the computation rate $\{\varrho_m^*\}_{\forall m}$ are respectively given by

$$\mathbf{w}^* = (\mathbf{A}_c \mathbf{x}\mathbf{x}^H \mathbf{A}_c^H + \sigma_0^2 \mathbf{I}_N)^{-1} \mathbf{a}_r(\theta_0), \tag{32}$$

$$\varrho_m^* = \frac{\nu_m (D_m^{\text{tot}} - \sum_{n \in \mathcal{N}} d_{mn})}{T_m - \frac{D_m^{\text{tot}}}{R_m^u}}, \forall m \in \mathcal{M}. \tag{33}$$

It can be identified that constraints (30) and (31) are difference of convex forms. To transform them into convex functions, we perform the first order Taylor expansion of $\mathbf{h}_m^H \mathbf{\Gamma}_m^{-1} \mathbf{h}_m$, for the τ-th iteration of the SCA, we obtain the lower bound as

$$\mathbf{h}_m^H \mathbf{\Gamma}_m^{-1} \mathbf{h}_m \geq \Omega_m^{\text{lb}} \triangleq \mathbf{h}_m^H (\mathbf{\Gamma}_m^{\tau-1})^{-1} \mathbf{h}_m - \mathbf{h}_m^H (\mathbf{\Gamma}_m^{\tau-1})^{-1} \left(\mathbf{\Gamma}_m - \mathbf{\Gamma}_m^{\tau-1}\right) (\mathbf{\Gamma}_m^{\tau-1})^{-1} \mathbf{h}_m, \tag{34}$$

where $\mathbf{\Gamma}_m^{\tau-1}$ denotes the solution obtained in the $(\tau-1)$th iteration and it can be expressed as

$$\mathbf{\Gamma}_m^{\tau-1} = (\mathbf{A}_s + \mathbf{A}_c)\, \mathbf{x}^{\tau-1} (\mathbf{x}^{\tau-1})^H \left(\mathbf{A}_s^H + \mathbf{A}_c^H\right) + \sum_{j \in \mathcal{M}, j \neq m} p_j \mathbf{h}_j \mathbf{h}_j^H + \sigma_0^2 \mathbf{I}_N. \tag{35}$$

Then, constraints (30) and (31) are replaced by the following two convex constraints

$$\frac{D_m^{\text{tot}}}{T_m - \frac{\nu_m (D_m^{\text{tot}} - \sum_{n \in \mathcal{N}} d_{mn})}{\varrho_m}} - \tilde{R}_m^u \leq 0, \forall m \in \mathcal{M}, \tag{36}$$

$$\frac{D_m^{\text{tot}}}{T_m - t_n - \frac{\nu_m d_{mn}}{\zeta_{mn}}} - \tilde{R}_m^u \leq 0, \forall m \in \mathcal{M}, \forall n \in \mathcal{N}, \tag{37}$$

where

$$\tilde{R}_m^u = B^d \log_2 \left(1 + p_m \Omega_m^{\text{lb}}\right). \tag{38}$$

With Eq. (20), constraint (25) is transformed into

$$\frac{1}{\gamma_n^{e,\max}} |\mathbf{\Theta}^H \mathbf{u}_n|^2 - \sigma_e^2 \leq \sum_{j \in \mathcal{N}, j \neq n} |\mathbf{\Theta}^H \mathbf{u}_j|^2 + |\mathbf{\Theta}^H \mathbf{v}_0|^2. \tag{39}$$

By performing the first order Taylor expansion of the right hand side in Eq. (39), for the τth iteration of the SCA, we obtain the lower bound as

$$\begin{aligned} \sum_{j \in \mathcal{N}, j \neq n} |\mathbf{\Theta}^H \mathbf{u}_j|^2 + |\mathbf{\Theta}^H \mathbf{v}_0|^2 \geq \Psi_n^{\text{lb}} \triangleq 2\text{Re}\{(\mathbf{\Theta}^H \mathbf{v}_0^\tau)^\dagger (\mathbf{\Theta}^H \mathbf{v}_0)\} - |\mathbf{\Theta}^H \mathbf{v}_0^\tau|^2 \\ + \sum_{j \in \mathcal{N}, j \neq n} \left(2\text{Re}\{(\mathbf{\Theta}^H \mathbf{u}_j^\tau)^\dagger (\mathbf{\Theta}^H \mathbf{u}_j)\} - |\mathbf{\Theta}^H \mathbf{u}_j^\tau|^2\right), \end{aligned} \tag{40}$$

where $\mathbf{u}_n^\tau$ and $\mathbf{v}_0^\tau$ denote the solutions obtained in the $(\tau-1)$th iteration. Then, constraint (25) can be replaced by the convex function as

$$\frac{1}{\gamma_n^{e,\max}}|\mathbf{\Theta}^H\mathbf{u}_n|^2 - \Psi_n^{\text{lb}} - \sigma_e^2 \leq 0, \forall n \in \mathcal{N}. \tag{41}$$

Then, we address nonconvex constraint (26). By using Lagrangian dual transform method, we introduce the auxiliary variables $\{\lambda_n\}_{\forall n}$ and rewrite R_n^d in Eq. (14) as

$$\bar{R}_n^d = B^d(1+\lambda_n)\mathbf{u}_n^H\mathbf{G}_n^H\mathbf{E}_n^{-1}\mathbf{G}_n\mathbf{u}_n + B^d\log_2(1+\lambda_n) - B^d\lambda_n, \tag{42}$$

where $\mathbf{E}_n$ is given by

$$\mathbf{E}_n = \mathbf{G}_n\mathbf{u}_n\mathbf{u}_n^H\mathbf{G}_n^H + \mathbf{\Lambda}_n. \tag{43}$$

It can be identified that $\bar{R}_n^d$ is a concave function of $\{\lambda_n\}_{\forall n}$ under the given $\{\mathbf{u}_n\}_{\forall n}$. The first derivative of $\bar{R}_n^d$ regarding $\{\lambda_n\}_{\forall n}$ is given by

$$\frac{\partial\bar{R}_n^d}{\partial\lambda_n} = B^d\mathbf{u}_n^H\mathbf{G}_n^H\mathbf{E}_n^{-1}\mathbf{G}_n\mathbf{u}_n - \frac{B^d\lambda_n}{(1+\lambda_n)}. \tag{44}$$

By using Sherman Morrison formula, Eq. (44) can be rewritten as

$$\begin{aligned}\frac{\partial\bar{R}_n^d}{\partial\lambda_n} &= -\frac{B^d\mathbf{u}_n^H\mathbf{G}_n^H\mathbf{\Lambda}_n^{-1}\mathbf{G}_n\mathbf{u}_n\mathbf{u}_n^H\mathbf{G}_n^H\mathbf{\Lambda}_n^{-1}\mathbf{G}_n\mathbf{u}_n}{(1+\mathbf{u}_n^H\mathbf{G}_n^H\mathbf{\Lambda}_n^{-1}\mathbf{G}_n\mathbf{u}_n)} \\ &\quad + B^d\mathbf{u}_n^H\mathbf{G}_n^H\mathbf{\Lambda}_n^{-1}\mathbf{G}_n\mathbf{u}_n - \frac{B^d\lambda_n}{(1+\lambda_n)} \\ &= \frac{B^d\mathbf{u}_n^H\mathbf{G}_n^H\mathbf{\Lambda}_n^{-1}\mathbf{G}_n\mathbf{u}_n}{(1+\mathbf{u}_n^H\mathbf{G}_n^H\mathbf{\Lambda}_n^{-1}\mathbf{G}_n\mathbf{u}_n)} - \frac{B^d\lambda_n}{(1+\lambda_n)}.\end{aligned} \tag{45}$$

Let $\frac{\partial\bar{R}_n^d}{\partial\lambda_n} = 0$, we can derive that the optimal solution of $\{\lambda_n\}_{\forall n}$ can be expressed as

$$\lambda_n^* = \mathbf{u}_n^H\mathbf{G}_n^H\mathbf{\Lambda}_n^{-1}\mathbf{G}_n\mathbf{u}_n. \tag{46}$$

Since Eq. (42) is still nonconvex, we further use multiple dimensional quadratic transformation method to rewrite $\bar{R}_n^d$ as

$$\tilde{R}_n^d = 2\sqrt{B^d(1+\lambda_n)}\text{Re}\{\mathbf{u}_n^H\mathbf{G}_n^H\mathbf{f}_n\} - \mathbf{f}_n^H\mathbf{E}_n\mathbf{f}_n + B^d\log_2(1+\lambda_n) - B^d\lambda_n, \tag{47}$$

where $\{\mathbf{f}_n\}_{\forall n} \in \mathbb{C}^{N_r\times 1}$ are the auxiliary vectors. By substituting Eq. (43) into Eq. (47), we obtain

$$\begin{aligned}\tilde{R}_n^d =& 2\sqrt{B^d(1+\lambda_n)}\text{Re}\{\mathbf{u}_n^H\mathbf{G}_n^H\mathbf{f}_n\} - |\mathbf{f}_n^H\mathbf{G}_n\mathbf{u}_n|^2 - \sum_{j\in\mathcal{N},j\neq n}|\mathbf{f}_n^H\mathbf{G}_n\mathbf{u}_j|^2 \\ &- |\mathbf{f}_n^H\mathbf{G}_n\mathbf{v}_0|^2 - \sigma_n^2||\mathbf{f}_n||_F^2 + B^d\log_2(1+\lambda_n) - B^d\lambda_n.\end{aligned} \tag{48}$$

According to the criterion of multiple dimensional quadratic transformation, the optimal solution of $\{\mathbf{f}_n\}_{\forall n}$ is given by

$$\mathbf{f}_n^* = \sqrt{B^d(1+\lambda_n)}\mathbf{E}_n^{-1}\mathbf{G}_n\mathbf{u}_n. \tag{49}$$

After the above operations, the nonconvex constraint (26) is equivalently transformed into

$$\tilde{R}_n^d \geq R_n^{d,\min}, \forall n \in \mathcal{N}. \tag{50}$$

We next address the fractional form of the objective function. By introducing the auxiliary variables $\{\varpi_{\theta_0}\}_{\theta_0\in\Phi}$ and using the quadratic transformation, the objective function of Problem (SCO) can be equivalently rewritten as

$$\max \min_{\theta_0\in\Phi} 2\varpi_{\theta_0}\sqrt{|\mathbf{w}^H\mathbf{A}_s\mathbf{x}|^2} - \varpi_{\theta_0}^2\mathbf{w}^H(\mathbf{A}_c\mathbf{x}\mathbf{x}^H\mathbf{A}_c^H + \sigma_0^2\mathbf{I}_N)\mathbf{w} \tag{51}$$

The optimal solution of ϖ_{θ_0} can be updated by

$$\varpi_{\theta_0}^* = \frac{\sqrt{|\mathbf{w}^H\mathbf{A}_s\mathbf{x}|^2}}{\mathbf{w}^H(\mathbf{A}_c\mathbf{x}\mathbf{x}^H\mathbf{A}_c^H + \sigma_0^2\mathbf{I}_N)\mathbf{w}}. \tag{52}$$

To tackle the *max-min* form of the objective function (51), we further introduce an auxiliary variable μ which satisfies

$$\mu \leq \min_{\theta_0\in\Phi} 2\varpi_{\theta_0}\sqrt{|\mathbf{w}^H\mathbf{A}_s\mathbf{x}|^2} - \varpi_{\theta_0}^2\mathbf{w}^H(\mathbf{A}_c\mathbf{x}\mathbf{x}^H\mathbf{A}_c^H + \sigma_0^2\mathbf{I}_N)\mathbf{w}. \tag{53}$$

Then, the objective function (51) can be equivalently transformed into

$$\max \ \mu \tag{54}$$

with the following constraint

$$2\varpi_{\theta_0}\sqrt{|\mathbf{w}^H\mathbf{A}_s\mathbf{x}|^2} - \varpi_{\theta_0}^2\mathbf{w}^H(\mathbf{A}_c\mathbf{x}\mathbf{x}^H\mathbf{A}_c^H + \sigma_0^2\mathbf{I}_N)\mathbf{w} \geq \mu, \forall\theta_0 \in \Phi. \tag{55}$$

Constraint (55) is still nonconvex. Thus, we perform the first order Taylor expansion of the first term of $|\mathbf{w}^H\mathbf{A}_s\mathbf{x}|^2$, we obtain its lower bound as

$$|\mathbf{w}^H\mathbf{A}_s\mathbf{x}|^2 \geq \psi^{\text{lb}} \triangleq 2\text{Re}\{(\mathbf{w}^H\mathbf{A}_s\mathbf{x}^\tau)^\dagger(\mathbf{w}^H\mathbf{A}_s\mathbf{x})\} - |\mathbf{w}^H\mathbf{A}_s\mathbf{x}^\tau|^2. \tag{56}$$

Based on the following operations, the surrogate problem for Problem (SCO) can be established as

(SCO-Sur): $\max \ \mu$

subject to: constraints (28), (29), (36), (37), (41), and (50),

$$-\varpi_{\theta_0}^2\mathbf{w}^H(\mathbf{A}_c\mathbf{x}\mathbf{x}^H\mathbf{A}_c^H + \sigma_0^2\mathbf{I}_N)\mathbf{w} + 2\varpi_{\theta_0}\sqrt{\psi^{\text{lb}}} \geq \mu, \forall\theta_0 \in \Phi, \tag{57}$$

$$R_n^{d,\min}t_n \geq \sum_{m\in\mathcal{M}} d_{mn}, \forall n \in \mathcal{N}, \tag{58}$$

variables: $\{\mathbf{u}_n\}_{\forall n}, \mathbf{v}_0, \mathbf{w}, \{d_{mn}\}_{\forall m,n}, \{t_n\}_{\forall n}, \{\lambda_n\}_{\forall n}, \{\mathbf{f}_n\}_{\forall n}, \{\varpi_{\theta_0}\}_{\forall\theta_0}, \{\varrho_m\}_{\forall m}$, and μ.

It can be identified that Problem (SCO-Sur) is a strict convex optimization problem, since the objective function is affine, and all constraints compose a convex feasible region. Therefore, we cam obtain the solution of Problem (SCO) by solving Problem (SCO-Sur) with CVX in an iterative manner. The details for solving Problem (SCO) are shown as follows.

Algorithm 1 : To solve Problem (SCO).

1: **Initialization:** Initialize $\{d_{mn}[0]\}_{\forall m,n}$, $\{\mathbf{u}_n[0]\}_{\forall n}$ and $\mathbf{v}_0[0]$. Set $k = 0$.
2: **repeat**
3: Set $k = k + 1$.
4: Update $\mathbf{w}[k]$ according to Eq. (32).
5: Update $\{\varrho_m[k]\}_{\forall m}$ according to Eq. (33).
6: Update $\{\lambda_n[k]\}_{\forall n}$ according to Eq. (46).
7: Update $\{\mathbf{f}_n[k]\}_{\forall n}$ according to Eq. (49).
8: Update $\{\varpi_{\theta_0}[k]\}_{\forall \theta_0}$ according to Eq. (52).
9: Solve Problem (SCO-Sur) with $\{\mathbf{w}[k]\}$, $\{\varrho_m[k]\}_{\forall m}$, $\{d_{mn}[k-1]\}_{\forall m,n}$, $\{\mathbf{u}_n[k-1]\}_{\forall n}, \mathbf{v}_0[k-1]$, $\{\lambda_n[k]\}_{\forall n}$, $\{\mathbf{f}_n[k]\}_{\forall n}$, and $\{\varpi_{\theta_0}[k]\}_{\forall \theta_0}$ by using CVX and obtain $\{d_{mn}[k]\}_{\forall m,n}$, $\{\mathbf{u}_n[k]\}_{\forall n}$, $\mathbf{v}_0[k]$, and $\{t_n\}_{\forall n}$.
10: **until** *Convergence*
11: Set $\{d^*_{mn} = d_{mn}[k]\}_{\forall m,n}$, $\{\mathbf{u}^*_n = \mathbf{u}_n[k]\}_{\forall n}$, $\mathbf{v}^*_0 = \mathbf{v}_0[k]$, $\{\varrho^*_m = \varrho_m[k]\}_{\forall m}$, $\{t^*_n = t_n[k]\}_{\forall n}$ and $\mathbf{w}^* = \mathbf{w}[k]$.
12: **Output:** $\{d^*_{mn}\}_{\forall m,n}$, $\{\mathbf{u}^*_n\}_{\forall n}$, $\mathbf{v}^*_0$, $\{\varrho^*_m\}_{\forall m}$, $\{t^*_n\}_{\forall n}$, $\mathbf{w}^*$.

4 Numerical Results

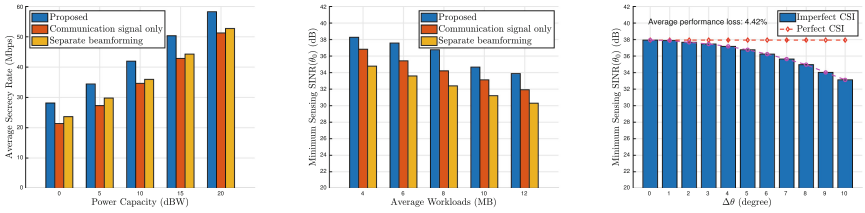

(a) Secrecy (b) Sensing performance (c) Robustness

Fig. 3. Performance advantages of our ISAC empowered secure computation offloading

We present numerical results to demonstrate the performance advantages of our ISAC empowered secure computation offloading in the integrated satellite-terrestrial network. We consider the tested scenario of $M = 4$ EUs and $N = 2$ BSs. We set $N_t = 10$ transmit antennas and $N_r = 15$ receive antennas. We

assume that the communication link between the LEO satellite and the terrestrial transceiver is dominated by the line of sight component. The channels between the satellite and terrestrial in this work are set according to [11]. Moreover, We set bandwidth $B^u = B^d = 10$ MHz, $\Delta\theta = 5^\circ$, $\epsilon_0 = 1 \times 10^{-28}$, and set $\sigma_0^2 = \sigma_n^2 = -80$ dBm.

To verify the performance advantages of the ISAC empowered secure computation offloading, we consider the following benchmarks for comparison.

- Communication signal only: In this benchmark scheme, we only use the communication signal as the integrated signal (i.e., without the dedicated sensing signal) for both sensing and offloading.
- Separate beamforming: In this benchmark scheme, we use the conventional separate design of the communication signal and the sensing signal.

Figure 3 demonstrates the performance superiority of our proposed approach. Figure 3(a) shows the average secrecy offloading rate of the LEO satellite with different power capacities. It can be seen that the average secrecy rate is increasing with respect to the value of the LEO satellite's power capacity $P_0^{\max}$. Figure 3(b) shows the minimum sensing performance within the eavesdropper's uncertain region under different average task workloads. It can be observed that the minimum sensing performance is decreasing with respect to the workloads due to the fact that the increased workloads result in more resources being allocated for computation offloading. The results in Figs. 3(a) and 3(b) verify that our proposed scheme outperforms the benchmark schemes in security. Figure 3(c) shows the minimum sensing performance with different uncertain regions. The red dashed line represents the case in which the satellite has perfect CSI about the eavesdropper. In particular, the average performance loss of our proposed scheme in the case of eavesdropper location uncertainty compared to the perfect eavesdropper CSI is marked at the top of Fig. 3(c). The results show that the average loss does not exceed 5%, which verifies the robustness of our scheme.

5 Conclusions

In this paper, we have proposed an ISAC empowered secure computation offloading in integrated satellite-terrestrial networks, in which the ISAC signal transmitted by the LEO satellite can be used for sensing the potential eavesdropper with an uncertain location while improving secrecy offloading transmission rates. We have proposed a joint optimization of the transmit beamforming, the receive beamforming, the computation offloading strategies and the associated allocations of communication and computing resources, with the aim of achieving the robust security of the network. Despite the nonconvexity of the formulated problem, we have proposed an efficient algorithm to obtain its solutions. In our future work, we will investigate the integration of quantum cryptographic techniques and covert communication methods within integrated satellite-terrestrial networks to further enhance security against sophisticated eavesdroppers.

Acknowledgement. This work was supported in part by National Natural Science Foundation of China under Grants 62122069, 62072490, and 62071431, in part by the Guangdong Basic and Applied Basic Research Foundation (2022A1515011287), in part by Science and Technology Development Fund of Macau SAR under Grant FDCT 0158/2022/A, and in part by MYRG-GRG2023-00083-IOTSC-UMDF.

References

1. Chen, Q., Meng, W., Quek, T.Q.S., Chen, S.: Multi-tier hybrid offloading for computation-aware IoT applications in civil aircraft-augmented SAGIN. IEEE J. Sel. Areas Commun. **41**(2), 399–417 (2023). https://doi.org/10.1109/JSAC.2022.3227031
2. Liu, Y., Chen, H.H., Wang, L.: Physical layer security for next generation wireless networks: theories, technologies, and challenges. IEEE Commun. Surv. Tutorials **19**(1), 347–376 (2017). https://doi.org/10.1109/COMST.2016.2598968
3. Liu, Y., et al.: Physical layer security assisted computation offloading in intelligently connected vehicle networks. IEEE Trans. Wireless Commun. **20**(6), 3555–3570 (2021). https://doi.org/10.1109/TWC.2021.3051772
4. Liu, Y., Ni, L., Peng, M.: A secure and efficient authentication protocol for satellite-terrestrial networks. IEEE Internet Things J. **10**(7), 5810–5822 (2023). https://doi.org/10.1109/JIOT.2022.3152900
5. An, K., Lin, M., Ouyang, J., Zhu, W.P.: Secure transmission in cognitive satellite terrestrial networks. IEEE J. Sel. Areas Commun. **34**(11), 3025–3037 (2016). https://doi.org/10.1109/JSAC.2016.2615261
6. Lin, Z., Lin, M., Champagne, B., Zhu, W.P., Al-Dhahir, N.: Secrecy-energy efficient hybrid beamforming for satellite-terrestrial integrated networks. IEEE Trans. Commun. **69**(9), 6345–6360 (2021). https://doi.org/10.1109/TCOMM.2021.3088898
7. Dou, C., Huang, N., Wu, Y., Qian, L., Quek, T.Q.S.: Sensing-efficient NOMA-aided integrated sensing and communication: a joint sensing scheduling and beamforming optimization. IEEE Trans. Veh. Technol. **72**(10), 13591–13603 (2023). https://doi.org/10.1109/TVT.2023.3277734
8. Yuan, W., Wei, Z., Li, S., Yuan, J., Ng, D.W.K.: Integrated sensing and communication-assisted orthogonal time frequency space transmission for vehicular networks. IEEE J. Sel. Top. Sig. Process. **15**(6), 1515–1528 (2021). https://doi.org/10.1109/JSTSP.2021.3117404
9. Lyu, Z., Zhu, G., Xu, J.: Joint maneuver and beamforming design for UAV-enabled integrated sensing and communication. IEEE Trans. Wireless Commun. **22**(4), 2424–2440 (2023). https://doi.org/10.1109/TWC.2022.3211533
10. Dou, C., Huang, N., Wu, Y., Qian, L., Quek, T.Q.S.: Channel sharing aided integrated sensing and communication: an energy-efficient sensing scheduling approach. IEEE Trans. Wireless Commun. **23**(5), 4802–4814 (2024). https://doi.org/10.1109/TWC.2023.3322680
11. Yin, Z., et al.: UAV-assisted physical layer security in multi-beam satellite-enabled vehicle communications. IEEE Trans. Intell. Transp. Syst. **23**(3), 2739–2751 (2022). https://doi.org/10.1109/TITS.2021.3090017